SACRP: A Spectrum Aggregation-Based Cooperative Routing Protocol for Cognitive Radio Ad-Hoc Networks

Shuyu Ping, Adnan Aijaz, *Member, IEEE*, Oliver Holland, and Abdol-Hamid Aghvami, *Fellow, IEEE*

***Abstract*—Cooperative routing and spectrum aggregation are two promising techniques for Cognitive Radio Ad-Hoc Networks (CRAHNs). In this paper, we propose a spectrum aggregation-based cooperative routing protocol, termed as SACRP, for CRAHNs. To the best of our knowledge, this is the first contribution on spectrum aggregation-based cooperative routing for CRAHNs. The primary objective of SACRP is to provide higher energy efficiency, improve throughput, and reduce network delay for CRAHNs. In this regard, we design the MAC and Physical (PHY) layer, and proposed different spectrum aggregation algorithms for cognitive radio (CR) users. We propose two different classes of routing protocols; Class A for achieving higher energy efficiency and throughput, and Class B for reducing end-to-end latency. Based on stochastic geometry approach, we build a comprehensive analytical model for the proposed protocol. Besides, the proposed protocol is compared with the state of the art cooperative and non-cooperative routing algorithms with spectrum aggregation. Performance evaluation demonstrates the effectiveness of SACRP in terms of energy efficiency, throughput, and end-to-end delay.**

***Index Terms*—Cognitive radio networks, cooperative routing, spectrum aggregation.**

I. Introduction

SPECTRUM scarcity is one of the primary bottlenecks for the development of future wireless communication systems. Under current spectrum allocation policies, the spectrum utilization efficiency in licensed spectrum at a particular time and location is very low [1]. The Federal Communications Commission (FCC) estimates the usage of assigned spectrum to be between 15% and 85% [2]. To address such inefficiency given limited spectrum availability, the FCC has approved solutions such as opportunistic usage of licensed spectrum such as TV white spaces [3]. Such solutions will be eventually realized through the adoption of Cognitive Radio (CR) [2], [4] technology, which is envisaged to increase spectrum utilization through dynamic spectrum access (DSA) technique, wherein unlicensed (CR) users opportunistically use licensed bands when not occupied [5]. Consequently, the utilization of spectrum can be greatly enhanced by opportunistic communication on licensed spectrum.

A. Motivation and Related Work

The traditional wireless techniques can only support the utilization of continuous spectrum resources. However, wide continuous spectrum bands are rarely available under the current situation of spectrum resources and the policy of stable licensed spectrum utilization. In this regard, *spectrum aggregation* [6] technique has been proposed to satisfy the increasing bandwidth demands. Recently, a number of studies (e.g., see [1], [7]–[11]) have focused on different spectrum aggregation algorithms for CR networks for increasing spectrum efficiency and throughputs. Such studies are generally based on an advanced wireless technique: *Discontiguous Orthogonal Frequency Division Multiplexing* (DOFDM) [12], which can switch off the sub-carriers occupied by primary users (PU) and thus, enables a single CR user to access several spectrum fragments simultaneously on the *Physical* (PHY) layer with only one Radio Front (radio transceiver). In [10], Aggregation Aware Spectrum Assignment Algorithm (AASA) is proposed based on a greedy algorithm, which aggregates spectrum fragments from low frequency to high frequency to satisfy the bandwidth requirements. AASA optimizes the spectrum assignment and maximizes the number of supported users. However, it assumes all the nodes have the same bandwidth requirements which is not practical. The authors in [8] provide a Maximum Satisfaction Algorithm (MSA) to allocate the spectrum bands under different bandwidth requirements for CR users. This algorithm always assigns the spectrum bands for the user with higher bandwidth requirement first, and can accommodate more users than AASA when the bandwidth requirements are different. A Channel Characteristic Aware Spectrum Aggregation (CCASA) algorithm has been proposed in [11], which combines Adaptive Modulation and Coding (AMC) [13] and spectrum aggregation to increase the network throughput under hardware constraints.

On the other hand, Cognitive Radio Ad-Hoc Networks (CRAHNs) have attracted much attention in the research community in recent years. Unlike either traditional CR networks or ad-hoc networks, CRAHNs provide a non-infrastructure support and spectrum heterogeneity based wireless network which raises unique issues and challenges. In [4], the authors summarize the unique features of CRAHNs and outline the

Manuscript received September 19, 2014; revised January 27, 2015 and April 8, 2015; accepted April 10, 2015. Date of publication April 17, 2015; date of current version June 12, 2015. This work has been supported by the Spectrum Overlay through Aggregation of Heterogeneous Dispersed Bands project, ICT-SOLDER, www.ict-solder.eu, FP7 grant agreement number 619687. The associate editor coordinating the review of this paper and approving it for publication was L. Badia.

The authors are with the Centre for Telecommunication Research, King's College London, London WC2R 2LS, U.K. (e-mail: shuyu.ping@kcl.ac.uk).

Color versions of one or more of the figures in this paper are available online at http://ieeexplore.ieee.org.

Digital Object Identifier 10.1109/TCOMM.2015.2424239

relevant research issues. An important issue is the design of routing protocols for CRAHNs. The authors of [14] review several adaptations of different kinds of on-demand routing protocols: AODV, DSR, and hybrid on-demand protocols for CRAHNs. They also investigate the challenges and issues of each routing protocol in CRAHNs. Recently, a number of studies (e.g., see [15]–[21]) have investigated routing protocols for CRAHNs. So far, two distinct types of routing protocols have been investigated: cooperative routing and non-cooperative routing protocols. A distributed CR routing protocol is proposed in [16] to specifically address the problems of PU receiver protection, service differentiation in CR routes, and joint spectrum-route selection. In [17], a cooperative routing protocol has been considered for achieving higher channel capacity gain. Due to spectrum heterogeneity characteristics, the channel which provides maximum capacity is selected for transmission in each direct link, and the node that can provide the maximum capacity gain is selected as the relay node for cooperative routing. Furthermore, the authors in [22] propose a heuristic algorithm for cooperative routing to solve the resource allocation problem, which is based on the metric of utility-spectrum ratio of transmission groups. The results demonstrate the improvement of the cooperative transmission over the direct transmission.

B. Contributions and Outline

Against this background, our objective in this paper is to design a spectrum aggregation-based routing protocol for CRAHNs. To the best of authors' knowledge, no routing protocol with spectrum aggregation exists in literature for CRAHNs. Our focus is specifically on the design of cooperative routing protocol as the cooperative approach provides an opportunity of enhancing the performance in terms of different metrics, compared to the non-cooperative approach. The proposed protocol is termed as SACRP (Spectrum Aggregation based Cooperative Routing Protocol) for CRAHNs. The main contributions of the paper can be summarized as follows.

- We begin our discussion with the spectrum aggregation framework for CRAHNs. This includes the design of PHY and MAC layer needed to aggregate different spectrum bands/channels. After this, we propose three different spectrum aggregation algorithms that allow a CR user to transmit data over aggregated bands/channels simultaneously with different objectives related to the utility of the CR network. The first algorithm minimizes the transmit power for CR users based on a rate demand. The second algorithm maximizes the aggregate channel capacity for a CR user. Finally, the third algorithm minimizes the end-to-end latency for the CR network.
- Based on the spectrum aggregation algorithms, we design a cooperative routing protocol, termed as SACRP. The proposed protocol uses two different routing classes with special emphasis on energy efficiency, network throughput, and end-to-end delay.
- A comprehensive analytical model for the proposed protocol is built using tools from stochastic geometry. We adopt Poisson Point Process (PPP) for modeling the location of CR nodes in our network and derive analytical expressions capturing different aspects of the proposed routing protocol including MAC layer collisions, average number of hops, end-to-end power, throughput and latency.
- To validate the analytical modeling, we conduct a comprehensive simulation-based performance evaluation. We also compare the performance of the proposed protocol with state of the art cooperative and non-cooperative routing protocols for CRAHNs with spectrum aggregation.

TABLE I
FREQUENTLY USED NOTATIONS AND SYMBOLS

Notation	Description
$\mathbb{P}_d$	Probability of detection
$\mathbb{P}_f$	Probability of false alarm
$\mathbb{P}_{acc}^j$	Probability of accessing the j^{th} cognitive channel
P_{max}	Maximum total transmit power for the CR node
$\mathcal{P}^a$	Maximum allowed transmit power of the channel
$P_{x,y}$	Transmit power for CR node x transmitting to CR node y
$\mathcal{P}_{i,j}$	Transmit power of the j^{th} channel of the i^{th} spectrum
R_d	Rate demand
$\mathcal{R}$	Transmission range
$C_{x,y}$	Channel capacity of link (x, y)
$\mathcal{C}_{i,j}$	Channel capacity of the j^{th} channel of the i^{th} spectrum
Θ	Throughput
Φ	Delay
T_s	Spectrum sensing duration
T	Transmission duration
T_e	Effective transmit time
χ	Channel status
ϵ	Maximum number of aggregated channels
$\mathcal{E}$	The expected transmission count
ρ	Probability of transmitting data through cooperative link
N_a	The number of available channels
N_A	The number of aggregated channels
N	Average number of hops of the routing protocol

The rest of the paper is organized as follows. In Section II, we provide the network architecture and system model. Section III focuses on the design of PHY and MAC layers needed for spectrum aggregation and the proposed spectrum aggregation algorithms. This is followed by the framework for the proposed spectrum aggregation-based cooperative routing protocol in Section IV. In Section V, analytical modeling of the proposed protocol has been carried out. A comprehensive performance evaluation has been conducted in Section VI. Finally, Section VII concludes the paper. Frequently used notations and symbols throughout the paper are given in Table I.

II. NETWORK ARCHITECTURE AND SYSTEM MODEL

We consider a CRAHN where nodes are randomly distributed within a specified region. Each node (CR user) is equipped with a single radio transceiver that can be tuned to any channel in the licensed/unlicensed spectrum. The radio transceiver uses *Frequency-aware OFDM* (FA-OFDM) [13] and *Signal Interpretation before Fourier Transform* (SIFT) techniques[1] to avoid cross-channel interference and aggregate channels of different spectrum bands, respectively. This allows

[1]SIFT technique is proposed in [23], which performs an efficient time-domain analysis of the raw signal to detect the presence of PU activity and determine its bandwidth.

the CR user to access multiple bands simultaneously with different transmit powers [24]. We assume that all CR users share one dedicated common control channel (CCC) for exchanging control information. Further, we assume N stationary PU transmitters (and hence N available spectrum bands) with known locations and maximum coverage ranges. Each spectrum band contains M channels. Thus, the total number of channels are represented as: $\mathbf{F} = [[f_{1,1}, \ldots, f_{1,M}], [f_{2,1}, \ldots, f_{2,M}], \ldots, [f_{N,1}, \ldots, f_{N,M}]]^T$.

The PU activity model for the j^{th} channel is given by a two state independent and identically distributed (i.i.d.) random process such that the duration of busy and idle periods is exponentially distributed with a mean of $\frac{1}{\mu^j_{ON}}$ and $\frac{1}{\mu^j_{OFF}}$, respectively. Let S^j_b denote the state that the j^{th} channel is busy (PU is active) with probability $\mathbb{P}^j_b = \frac{\mu^j_{OFF}}{\mu^j_{ON}+\mu^j_{OFF}}$, and S^j_i the state that the j^{th} channel is idle with probability $\mathbb{P}^j_i$, such that $\mathbb{P}^j_i + \mathbb{P}^j_b = 1$. We assume that a node employs energy detection technique [25] for primary signal detection wherein it compares the received energy (E) with a predefined threshold (σ) to decide whether the j^{th} channel is occupied or not i.e.,

$$Sensing\ Decision = \begin{cases} S^j_b & \text{if} \quad E \geq \sigma \\ S^j_i & \text{if} \quad E < \sigma \end{cases} . \ j \in \mathbf{F} \tag{1}$$

The two principle metrics in spectrum sensing are the detection probability $(\mathbb{P}_d)$, and the false alarm probability $(\mathbb{P}_f)$. A higher detection probability ensures better protection to incumbents, whereas a lower false alarm probability ensures efficient utilization of the channel. As per [26], false alarm and detection probabilities for the j^{th} channel can be expressed as follows.

$$\mathbb{P}^j_f = Pr\left\{E \geq \sigma | S^j_i\right\} = \frac{1}{2} Erfc\left(\frac{1}{\sqrt{2}} \frac{\sigma - 2n_j}{\sqrt{4n_j}}\right), \tag{2}$$

$$\mathbb{P}^j_d = Pr\left\{E \geq \sigma | S^j_b\right\} = \frac{1}{2} Erfc\left(\frac{1}{\sqrt{2}} \frac{\sigma - 2n_j\left(\gamma_j + 1\right)}{\sqrt{4n_j\left(2\gamma_j + 1\right)}}\right), \tag{3}$$

where $Erfc(\cdot)$ is the complementary error function, and γ_j and n_j denote the signal-to-noise ratio (SNR) of the primary signal and the bandwidth-time product for the j^{th} channel, respectively.

We are interested in probability of accessing the cognitive channel. The CR users can only use the licensed channel in the absence of PU activity. However, in practice, there can be an element of inaccuracy in spectrum sensing. Let $\mathbb{P}^j_{acc}$ denote the probability of accessing the jth cognitive channel which can be evaluated considering the following cases: (i) when S^j_b and the node misses to detect it; (ii) when S^j_i and no false alarm is generated. Hence $\mathbb{P}^j_{acc}$ is given by

$$\mathbb{P}^j_{acc} = \mathbb{P}^j_b \left(1 - \mathbb{P}^j_d\right) + \mathbb{P}^j_i \left(1 - \mathbb{P}^j_f\right) . \ j \in \mathbf{F} \tag{4}$$

It can be easily verified that under perfect spectrum sensing conditions i.e., $\mathbb{P}^j_d = 100\%$ and $\mathbb{P}^j_f = 0\%$, (4) reduces to $\mathbb{P}^j_i$, which is intuitive.

III. Spectrum Aggregation for CRAHNs

In this section, we design the PHY and MAC layer for spectrum aggregation for CRAHNs. This is followed by our proposed spectrum aggregation algorithms.

A. PHY Layer for Spectrum Aggregation

To aggregate multiple channels from different spectrum bands, each CR node has to perform a multiple-channel spectrum sensing operation for the licensed spectrum bands. We assume that the CR user has this capability of sensing multiple channels periodically. It is assumed that each CR node maintains a *Channel Status Table* (CST), $\mathbf{X}$, which represents the status of the licensed spectrum bands based on the spectrum sensing results such that

$$\mathbf{X} = \begin{bmatrix} \chi_{11} & \chi_{12} & \cdots & \chi_{1M} \\ \chi_{21} & \chi_{22} & \cdots & \chi_{2M} \\ \vdots & \ddots & \vdots & \\ \chi_{N1} & \chi_{N2} & \cdots & \chi_{NM} \end{bmatrix}_{N \times M}, \quad \chi_{i,j} \in \{0, 1\} \tag{5}$$

where $\chi_{i,j}$ denotes the channel status on the jth channel of the i^{th} spectrum. If $\chi_{i,j} = 1$, the channel is available for CR nodes, otherwise, it is not. The CST will be updated periodically with spectrum sensing.

In general, the spectrum for CR users is fragmented due to fixed allocation of PUs in different bands. The size of each fragment can vary among different bands/channels. We assume that nodes in our CR network employ the SIFT technique for detecting available bands/channels with different bandwidths.

On the PHY layer, the selected channels are aggregated and the split data packets (as discussed in the next Section on MAC layer design) are carried by different carriers with different transmit powers or transmit rates. To achieve this, FA-OFDM technique is used on both transmitter and receiver sides. As shown in Fig. 1(b), unlike traditional OFDM, FA-OFDM uses independent modulation and coding schemes for each OFDM channel based on its individual received signal-to-noise ratio (SNR). Therefore, different transmit rates and different transmit powers can be used on different channels.

B. MAC Layer Design for Spectrum Aggregation

The MAC frame structure in a CR network consists of a sensing slot (T_s) and a transmission slot (T). In periodic spectrum sensing scenarios, there is a possibility of causing harmful interference to PUs due to imperfect spectrum sensing in practice. This interference is quantified in terms of *Interference Ratio* (IR), defined as the expected fraction of ON duration of PU transmission interrupted by the transmission of secondary users and is given for the j^{th} channel as follows [27].

$$IR_j = \left(1 - \mathbb{P}^j_d\right) \mathbb{P}^j_b + \mathbb{P}^j_i \left(1 - \mathbb{P}^j_f\right) + e^{-\mu T} \left(\mathbb{P}^j_f - \mathbb{P}^j_d\right), \tag{6}$$

where $\mu = \max(\mu^j_{ON}, \mu^j_{OFF})$. We assume that the nodes in our network employ optimal transmission time that maximizes the throughput of the secondary network subject to an interference constraint i.e., $IR_j \leq IR^j_{max}$, where IR^j_{max} denotes the

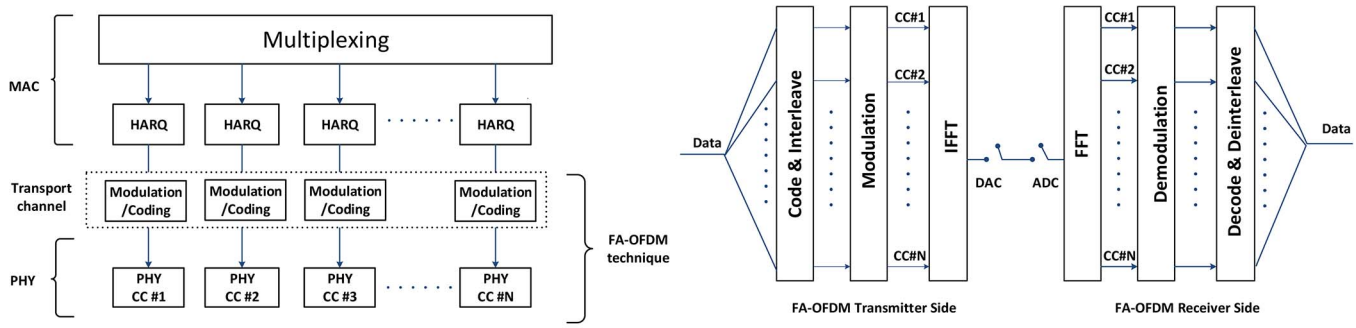

Fig. 1. (a) MAC and PHY layer structures for spectrum aggregation (HARQ refers to Hybrid Automatic Repeat Request), (b) PHY layer design based on FA-OFDM technique (adapted from [13]).

maximum tolerable interference ratio on the j^{th} channel. This transmission time is given for the j^{th} channel as follows.

$$T_j = \mu^{-1}\left[\ln \mathbb{P}_i^j - \ln\left(\mathbb{P}_i^j \mathbb{P}'_d + \mathbb{P}_b^j\left(1-\mathbb{P}'_d\right) - IR_{max}^j\right) + \ln\left(2\mathbb{P}'_d - 1\right)\right], \quad (7)$$

where $\mathbb{P}'_d$ is the detection probability threshold, defined as the detection probability at SNR level as low as γ_{min}, where γ_{min} is specified by the regulator. e propose spectrum aggregation algorithms for SACRP in which the data packets are split on the MAC layer before being transmitted on the PHY layer, as shown in Fig. 1(a). The transport channel provides modulation and coding operation on data packets, connecting MAC and PHY layers. Before that, each pair of nodes[2] completes exchanging control packets, which include Ready-To-Send (*RTS*), Clear-To-Send (*CTS*), and Reservation (*RES*). After exchanging control information, the set of aggregated channels from multiple spectrum bands and the transmission power of each channel can be determined. Thus the transmission involving spectrum aggregation can be set up between the source and destination node pair. The MAC layer transmission process is described as follows:

- *RTS Packet*: According to the multiple-channel spectrum sensing result, the *RTS* packet is sent from the source to the destination over all available channels.
- *CTS PACKET*: For each available channel, the destination node calculates the received SNR[3] after the *RTS* packet received. The destination node performs the spectrum selection operation to select the best set of channels from multiple spectrum bands based on their received SNRs. After that, a *CTS* packet will be sent back to the source node over the CCC. It contains the information about the selected channels $\mathcal{F} = \{f_1^s, f_2^s \ldots f_{N_A}^s\}$ as well as the required transmit power $\mathcal{P}_{tx}$ and transmission rate R_{tx} (discussed in the next section).
- *RES Packet*: If the source node receives the *CTS* packet, it will send a *RES* packet to confirm the successful reception of the *CTS* packet and to notify its neighbor nodes about the transmission. The *RES* contains the same information as the *CTS* packet.
- *Data packets transmission*: After exchanging control information, the source and destination nodes switch to the selected channels and start transmitting data packets. The data packets are split over the aggregated channels (e.g., if there are L_{data} data packets and N_A number of aggregated channels, the data packets per channel would be $\lceil \frac{L_{data}}{N_A} \rceil$). The data packets are transmitted simultaneously on different carriers with different transmit powers or rates. After receiving data packets, the destination node sends an *ACK* packet to the source node to confirm the reception of data packets.

It should be noted that a collision for control packets may occur owing to simultaneous transmission from multiple nodes in a multi-user scenario. We assume that a CR node takes a random back-off after a collision. The back-off taken by a CR node, in terms of back-off time slots, after the i^{th} collision is randomly distributed in the interval $[1, 2, \ldots, \kappa]$, where $\kappa = 2^i - 1$ denotes the upper bound on the back-off time slots. A detailed analysis of the collision scenario has been conducted in Section V.

Last, but not the least, the MAC and PHY layer design has been summarized as Algorithm 1.

C. Proposed Spectrum Aggregation Algorithms

In this section, we propose three different spectrum aggregation algorithms to meet the energy efficiency, throughput and end-to-end delay requirements of the secondary network, respectively.

Algorithm I: We aim to calculate the minimum transmission power for each CR user based on a rate demand. This is achieved by adapting the channel capacity given by Shannon's Theorem. The capacity of the link between CR users x and y over the k^{th} channel is given by

$$C_{x,y}^k = W_{x,y}^k \log_2\left(1 + SNR_k^y\right), \quad (8)$$

where $W_{x,y}^k$ is the potential bandwidth of the k^{th} channel, SNR_k^y is received SNR at node y, which is given by $SNR_k^y = \frac{P_{x,y}^k |h_{x,y}|^2}{\delta^2}$ such that $P_{x,y}^k$ is the transmit power of x^{th} node to

[2]The source and destination nodes in this case refer to the sending and receiving nodes within 1-hop vicinity.

[3]The SNR is the ratio of the signal power to the noise power which is given by [13] : $SNR_{i,j} = \frac{\mathcal{P}_{i,j}^{rx}}{N_0} - 1$, where $\mathcal{P}_{i,j}^{rx}$ is the received power over the j^{th} channel of spectrum i and N_0 is the noise power.

Algorithm 1: PHY AND MAC LAYER DESIGN FOR SPECTRUM AGGREGATION

The source node S performs multiple-channel spectrum sensing for all $\mathbf{F}$ channels in sensing slot T_s, and updates the CST $\mathbf{X}$
for $i = 1 : N$ **do**
  for $j = 1 : M$ **do**
    if $\chi_{i,j} \neq 0$ **then**
      S sends a *RTS* packet to node D over this channel;
      Node D calculates $SNR_{i,j} = \frac{\mathcal{P}_{i,j}^{rx}}{N_0} - 1$
    end
  end
end
Node D sends back a *CTS* packet containing $\{f_1^s, f_2^s \dots f_{N_A}^s\}$ over the CCC;
Node S sends the *RES* packet before data transmission.
for *j=1:* N_A **do**
  FA-OFDM provides different modulation and coding based on the SNR of each channel, and $\lceil \frac{L_{data}}{N_A} \rceil$ of data is transmitted simultaneously by node S.
  if *data packet received (by node D)* **then**
    return ACK
    else
      Node S re-transmits the packet
    end
  end
end

the y^{th} node over the k^{th} channel, δ^2 is the noise power and $h_{x,y} = F_{x,y}^k \sqrt{1/L_{x,y}}$ is the channel coefficient, where $F_{x,y}^k$ is the fading coefficient of the channel while $L_{x,y}$ is the pathloss.

For each CR user, we assume a minimum requested rate demand R_d. Thus the channel capacity should satisfy the following condition.

$$C_{x,y}^k = W_{x,y}^k \log_2 (1 + SNR_k^y) \geq R_d \tag{9}$$

Using the expression for SNR and solving for transmit power P, we obtain

$$P_{x,y}^k \geq \frac{\left(2^{\frac{R_d}{W_{x,y}^k}} - 1\right) \delta^2}{|h_{x,y}|^2}. \tag{10}$$

The potential bandwidth of the k^{th} channel for transmission between CR users x and y is obtained as follows.

$$W_{x,y}^k = \mathbb{P}_{acc}^k B_k, \tag{11}$$

where B_k is the bandwidth of the k^{th} channel. Note that the potential bandwidth actually provides the usable bandwidth since CR users access a channel with certain probability given by (4).

Thus, the minimum required transmit power from the CR node x to the node y over the k^{th} channel is given by

$$P_{x,y}^{min,k} = \frac{\left(2^{\frac{R_d}{\mathbb{P}_{acc}^k B_k}} - 1\right) \delta^2}{|h_{x,y}|^2}. \tag{12}$$

Similarly, the minimum transmit power for all $\mathbf{F}$ channels can be calculated and represented as a matrix: $\mathcal{P} = [[\mathcal{P}_{1,1}, \dots, \mathcal{P}_{1,M}], [\mathcal{P}_{2,1}, \dots, \mathcal{P}_{2,M}], \dots, [\mathcal{P}_{N,1}, \dots, \mathcal{P}_{N,M}]]^T$. The spectrum aggregation algorithm is represented as an optimization problem, given as follows.

$$\begin{aligned}
P_1: \quad & \min \sum_{i=1}^{N}\sum_{j=1}^{M} \mathcal{P}_{i,j}\chi_{i,j} \\
s.t. \quad & (a) \quad \mathcal{P}_{i,j} \leq \mathcal{P}_{i,j}^a, \quad \forall i \in N, \quad \forall j \in M \\
& (b) \quad \sum_{i=1}^{N}\sum_{j=1}^{M} \mathcal{C}_{i,j}\chi_{i,j} \geq R_d \\
& (c) \quad \sum_{i=1}^{N}\sum_{j=1}^{M} \chi_{i,j} \leq \epsilon \\
& (d) \quad \sum_{i=1}^{N}\sum_{j=1}^{M} \mathcal{P}_{i,j}\chi_{i,j} \leq P_{max} \\
& (e) \quad \chi_{i,j} \in \mathbf{X}, \quad \forall i \in N, \quad \forall j \in M
\end{aligned} \tag{13}$$

where $\mathcal{P}_{i,j}^a$ is the maximum allowed transmit power of the j^{th} channel of the i^{th} spectrum, P_{max} is the maximum total transmit power for a CR node, ϵ is the maximum number of channels that can be aggregated by the CR node due to the hardware constraints. The constraint (13a) ensures that the transmit power of each aggregated channel is limited by $\mathcal{P}_{i,j}^a$ to avoid interference to PUs. The constraint (13b) ensures that the total capacity of the aggregated channels must satisfy the minimum rate demand R_d. Lastly, the constraint (13d) ensures that the maximum transmit power constraint for a CR node is met.

Algorithm II: The aim of this algorithm is to maximize the aggregated channel capacity for a CR node. Using (8), the channel capacity of all $\mathbf{F}$ channels is represented as a matrix: $\mathbf{C} = [[\mathcal{C}_{1,1}, \dots, \mathcal{C}_{1,M}], [\mathcal{C}_{2,1}, \dots, \mathcal{C}_{2,M}], \dots, [\mathcal{C}_{N,1}, \dots, \mathcal{C}_{N,M}]]^T$. The spectrum aggregation algorithm is represented as the following optimization problem.

$$\begin{aligned}
P_2: \quad & \max \sum_{i=1}^{N}\sum_{j=1}^{M} \mathcal{C}_{i,j}\chi_{i,j} \\
s.t. \quad & (a) \quad \mathcal{P}_{i,j} \leq \mathcal{P}_{i,j}^a, \quad \forall i \in N, \quad \forall j \in M \\
& (b) \quad \sum_{i=1}^{N}\sum_{j=1}^{M} \mathcal{P}_{i,j}\chi_{i,j} \leq P_{max} \\
& (c) \quad \sum_{i=1}^{N}\sum_{j=1}^{M} \chi_{i,j} \leq \epsilon \\
& (d) \quad \sum_{i=1}^{N}\sum_{j=1}^{M} \mathcal{C}_{i,j}\chi_{i,j} \geq R_d \\
& (e) \quad \chi_{i,j} \in \mathbf{X}, \quad \forall i \in N, \forall \quad \forall j \in M
\end{aligned} \tag{14}$$

Note that the constraints have similar meaning and significance as in the optimization problem (13).

Algorithm III: The aim of this algorithm is to minimize the end-to-end latency for the CR network. In CR networks, the CR users perform spectrum sensing (with the duration of T_s) at periodic intervals to update the spectrum occupancy information on CSTs. For energy detection based spectrum sensing, the adjacent CR users must be silenced during the

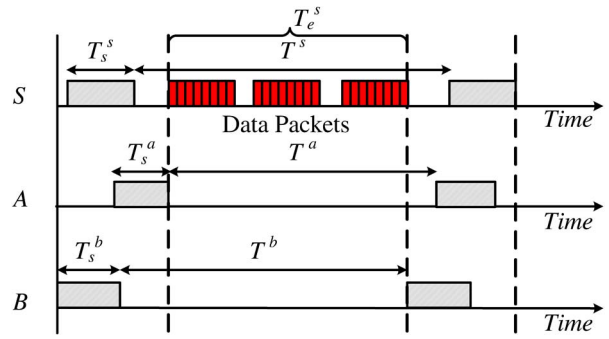

Fig. 2. The effective transmission time T_e^s for the CR node S with its two neighbors A and B.

sensing period. Hence, a delay arises when CR users have to stop their transmissions due to the enforcement of silence period. The effective transmit duration [16] for which the transmission is allowed at a candidate forwarding node, over a given channel, is an important criterion for the end-to-end delay of the CR network. Fig. 2 depicts the effective transmit time (T_e^S) for the node S. It is clear that the T_e^S is reduced due to the enforcement of silence period arising from the periodic spectrum sensing by neighboring nodes A and B.

Using Fig. 2 the effective transmit time of node S is calculated as follows.

$$T_e^S = \max\left\{T_s^i + T^i\right\} - \bigcup\left\{T_s^i\right\}, \tag{15}$$

where $\max\{T_s^i + T^i\}$ represents the maximum duration of the sensing and transmission time among all the neighbors of S and $\bigcup\{T_s^i\}$ is the cumulative duration of silence period. Note that T^i (for the i^{th} neighbor) is given by (7).

Recall that (4) provides the probability of accessing a cognitive channel. Hence, the total effective transmit time of node S on the k^{th} channel is given by

$$T_{E_k}^S = \mathbb{P}_{acc}^k T_e^S \tag{16}$$

To reduce the end-to-end latency, the channels which provide the maximum effective time must be aggregated by the CR node S. Therefore, the spectrum aggregation algorithm can be represented as the following optimization problem.

$$\begin{aligned}
P_3: \quad & \max \quad \sum_{i=1}^{N}\sum_{j=1}^{M} T_{E_{(i,j)}}\chi_{i,j} \\
s.t. \quad & (a) \quad \mathcal{P}_{i,j} \le \mathcal{P}_{i,j}^a, \quad \forall\, i \in N, \quad \forall\, j \in M \\
& (b) \quad \sum_{i=1}^{N}\sum_{j=1}^{M} \mathcal{P}_{i,j}\chi_{i,j} \le P_{max} \\
& (c) \quad \sum_{i=1}^{N}\sum_{j=1}^{M} \mathcal{C}_{i,j}\chi_{i,j} \ge R_d \\
& (d) \quad \sum_{i=1}^{N}\sum_{j=1}^{M} \chi_{i,j} \le \epsilon \\
& (e) \quad \chi_{i,j} \in \mathbf{X}, \quad \forall\, i \in N, \quad \forall\, j \in M
\end{aligned} \tag{17}$$

Note that the constraints have similar meaning and significance as in the optimization problem (13).

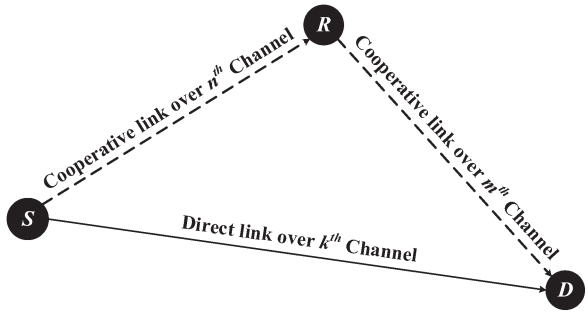

Fig. 3. Cooperative transmission in CRAHNs.

IV. SACRP Framework

In this section, we provide the framework for our proposed protocol, termed as SACRP. Our route selection algorithm is based on the shortest path selection. Initially, the source node sends a *route request* (RREQ) packet to the destination over the CCC. Each node along the packet forwarding path updates three fields in the RREQ. The first is the $\langle spect \rangle$ field which contains the aggregated channels of each hop, the second is the $\langle hop \rangle$ field which calculates the hop count of the path, and the third is the $\langle relay \rangle$ field which contains the relay node of each hop. When receiving the first RREQ packet, the destination node sets up a timer Δt to wait for receiving the same RREQ packets from other paths. From all received RREQ packets, the destination node selects the best path which has the minimum hop count as the direct path. For each hop of the direct path, the relay node is selected. SACRP considers two classes of routing protocols based on relay node selection: *Class A* for energy efficiency and throughput maximization, and the *Class B* for minimizing the end-to-end delay. After that the destination node sends a *route reply* (RREP) packet along the selected path over the CCC.

Class A: As mentioned above, the minimum required transmit powers for the aggregated channels are determined by (13). We assume that the required data rate R_d is fixed for each hop from the source to the destination. Considering a cooperative transmission as shown in Fig. 3, we propose to use the relay node r if and only if the cumulative minimum transmission power of the cooperative links (s, r) and (r, d) is less than that of the direct link (s, d). This condition is given by

$$\text{if and only if,} \quad P_{s,d} > P_{s,r} + P_{r,d}, \tag{18}$$

where $P_{s,d}$ is the minimum transmission power of the direct link (s, d), $P_{s,r}$ is the minimum transmission power of the cooperative link (s, r), and $P_{r,d}$ is the minimum transmission power of the cooperative link (r, d). If there are multiple relay nodes satisfying the condition (18), SACRP will select the one which provides the maximum cooperative gain.

The same process continues from the source to the destination. The selected path from the source node S to the destination node D is denoted as $Path = \{S, node1, node2, \ldots, D\}$. The total transmit power of link (i, j) by involving cooperative routing is given by

$$P_{i,j}^{tx} = (1-\rho)P_{i,j} + \rho\left(P_{i,r} + P_{r,j}\right), \tag{19}$$

where ρ is the probability of transmitting data over cooperative links. The total transmission power from S to D can be obtained by

$$P_{S,D}^{tx} = \sum_{i=S,\ldots,(D-1)}^{j=i+1} \left\{P_{i,j}^{tx}\right\} \tag{20}$$

Similarly a relay node is selected, if it provides higher channel capacity than the direct link. The capacity of a cooperative link over a given channel has been evaluated in [17], [18]. However, these studies assume that both direct link and cooperation links are using the same channel, which is rather unrealistic for CRAHNs. In CRAHNs, the relay node may use different channel from the direct link (as shown in Fig. 3). Thus, the capacity of the cooperative link over different channels is given by

$$C_{s,r,d} = \min\left\{W_{s,r}^{n}\log_2\left(1+SNR_{s,r}^{n}\right), W_{r,d}^{m}\log_2\left(1+SNR_{r,d}^{m}\right)\right\} \tag{21}$$

The relay node selection condition is given by

$$\text{if and only if,} \quad C_{s,r,d} > C_{s,d} \tag{22}$$

Hence, the total capacity of link (i,j) is represented by

$$C_{i,j}^{t} = (1-\rho)C_{i,j} + \rho\, C_{i,r,j} \tag{23}$$

For multi-hop network, the total capacity from the S to D of the selected path is given by

$$\sum_{i=S,\ldots,(D-1)}^{j=i+1} \left\{C_{i,j}^{t}\right\} \tag{24}$$

Class B: The end-to-end delay in a multi-hop network depends on the hop count and the number of retransmissions at each hop. We use *expected transmission count* (ETX) [28] as the default metric for relay node selection. The ETX of link from node s to node d is given by $\mathcal{E}_{s,d} = 1/p_{s,d}^{ss}$, where $p_{s,d}^{ss}$ is the probability of node d successfully receiving a transmission from node s. The ETX of a link will be measured and updated continuously, once the link starts to carry data traffic. For a direct link (s,d), if there is a node r providing smaller ETX than that of the direct link, it will be selected as the relay node. This condition is given as follows.

$$\text{if and only if,} \quad \mathcal{E}_{s,d} > \mathcal{E}_{s,r} + \mathcal{E}_{r,d}, \tag{25}$$

where $\mathcal{E}_{s,d}$ is the ETX of the direct link (s,d), $\mathcal{E}_{s,r}$ is the ETX of the cooperative link (s,r) and $\mathcal{E}_{r,d}$ is the ETX of the cooperative link (r,d).

The total delay of a link (s,d) with the relay node r is given as follows.

$$\Phi_{s,r,d} = (1-\rho)\mathcal{E}_{s,d}\,\Phi_{s,d} + \rho\left(\mathcal{E}_{s,r}\,\Phi_{s,r} + \mathcal{E}_{r,d}\,\Phi_{r,d}\right), \tag{26}$$

where $\Phi_{s,d}$ is the delay of direct link (s,d) for single transmission, $\Phi_{s,r}$ is the delay of cooperative link (s,r) and $\Phi_{r,d}$ is the delay of cooperative link (r,d). Similarly, the delay for multi-hop network is given by

$$\sum_{i=S,\ldots,(D-1)}^{j=i+1} \left\{\Phi_{i,j}\right\} \tag{27}$$

It should be noted that there is a possibility that a relay node is selected by multiple CR users. However, at any time instant, only one pair of CR users (sender and receiver nodes) can use the relay node for transmission. This is due to the fact that the proposed MAC layer design ensures that only one sender-receiver pair is active at any time instant.

Algorithm 2: PROPOSED SACRP FRAMEWORK

Input: *Source*: S, *Destination*: D, R_d, $\mathcal{P}^a$, P_{Max}, ϵ
Output: *Route*: $Path$
while $S \longrightarrow D$ **do**
  Node S sends the RREQ packet over the CCC;
end
if *Node D receives the first RREQ packet* **then**
  set a timer $\triangle t$
  if $t \leq \triangle t$ **then**
    Node D continues receiving RREQ packets
  end
  if $t > \triangle t$ **then**
    Node D stops receiving RREQ packets
  end
end
Node D compares the received RREQ packets and selects the route $Path$ which has the minimum number of hops;
for *each hop* $(i,j) \in Path$ **do**
  if *class A* **then**
    if *for energy efficiency* **then**
      the best channels are selected by (13), the relay node is selected by (18).
    end
    if *for throughput* **then**
      the best channels are selected by (14), the relay node is selected by (22).
    end
  end
  if *class B* **then**
    the channels are selected by (17), the relay node is selected by (25).
  end
end
return *RREP packet with* $Path$

V. ANALYTICAL MODEL FOR SACRP

In this section, we provide an analytical model for our proposed cooperative routing protocol. We adopt tools from stochastic geometry to develop the analytical model. In practice, nodes in an ad-hoc network are randomly distributed. Therefore, for the sake of developing a realistic model, we adopt the Poisson Point Process (PPP) for modeling the location of CR nodes in our network.[4] We assume that nodes are distributed according the PPP in an Euclidean plane with intensity λ.

A. Analysis of the Collision Scenario for Control Packet Transmission

In this section, we analyse the collision scenario for the transmission of control packets on the MAC layer. As shown in Fig. 4, a collision may happen when multiple CR nodes

[4]Recently, a number of studies have employed the PPP for modeling random ad-hoc networks [29]–[31]

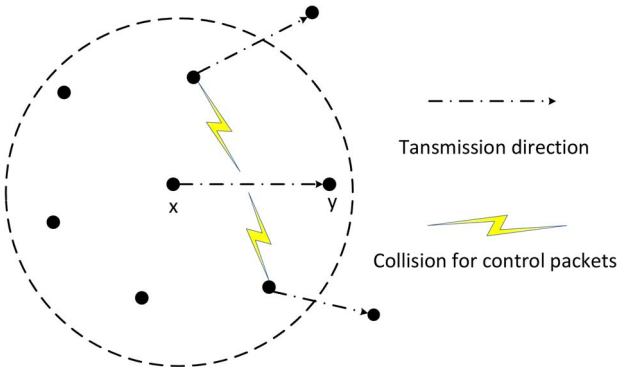

Fig. 4. The collision scenario for the control packets.

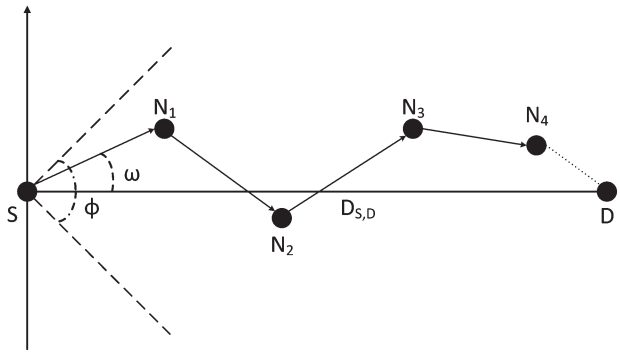

Fig. 5. The routing model with the source node at the origin and the x-axis pointing in the direction towards the destination node within a sector ϕ. ω is the angle between the x-axis and the path between nodes S and N_1.

transmit control packets over the same channel at the same time. We need to calculate the probabilities of a series of collisions, including *RTS*, *CTS*, and *RES* packets collisions.

1) Collision of RTS Packets: As the *RTS* packets are transmitted over all available channels, the collision may occur on one or more channels when one of the neighbors (interfering nodes) of the sender start transmission at the same time. The probability of *RTS* collision, denoted by $\mathbb{P}_{RTS}$, is given by

$$\mathbb{P}_{RTS} = 1 - (1-\tau)^{N_a\left(\lambda\pi\mathcal{R}^2-1\right)}, \tag{28}$$

where τ denotes the probability that the collision occurs on a single channel, λ is the CR node density, $\mathcal{R}$ is the transmission range of CR nodes, and N_a denotes the number of available channels based on the multi-channel spectrum sensing results in (5). Note that $\lambda\pi\mathcal{R}^2 - 1$ denotes the number of neigbors of a sender node.

Since N_a is a random variable, we need to find its expected value. The probability density function (pdf) of N_a is given by

$$f_{N_a}(n) = \binom{NM}{n} \left(\mathbb{P}^j_{acc}\right)^n \left(1-\mathbb{P}^j_{acc}\right)^{NM-n}, \tag{29}$$

where $\mathbb{P}^j_{acc}$ is given by (4) and NM is the total number of channels. Hence, the expected value of N_a can be calculated as

$$\mathbb{E}[N_a] = \sum_{N_a=1}^{NM} \binom{NM}{N_a} \left(\mathbb{P}^j_{acc}\right)^{N_a} \left(1-\mathbb{P}^j_{acc}\right)^{NM-N_a}. \tag{30}$$

2) Collision of CTS Packets: Since the *CTS* packet is sent by the receiving node over the CCC, a collision may occur when the nodes located in the transmission range of the receiving node start their transmissions at the same time. The probability of *CTS* collision is given by

$$\mathbb{P}_{CTS} = 1 - (1-\tau)^{\lambda\pi\mathcal{R}^2-1}. \tag{31}$$

3) Collision of RES Packets: Similarly, the collision for the *RES* packet occurs when the interference nodes initiate their transmissions during the RES packet transmission process on the CCC. The probability of *RES* collision is given by

$$\mathbb{P}_{RES} = 1 - (1-\tau)^{\lambda\pi\mathcal{R}^2-1}. \tag{32}$$

B. Analysis of the Routing Protocol

As our model is based on stochastic geometry approach for routing in random networks, we refer the interested reader to [32] for preliminaries. For analysis, we only consider Rayleigh fading channel. The fading coefficient of the k^{th} channel from a CR node x to a CR node y is denoted by $F^k_{x,y}$ such that $|F^k_{x,y}|^2$ is Exponentially distributed with mean $1/\mu$.

In SACRP, the objective is to find the path which has the minimum number of hops to destination. For each hop of the route, a relay node may be selected with different requirements. The model of the route selection can be considered as the farthest neighbor (within the transmission range) routing in the direction of the destination, as shown in Fig. 5.

Firstly, we determine the average number of hops towards destination. For this purpose, let $D_{S,D}$ denote the distance between the source and the destination node. The pdf of the distance to the farthest neighbor from a sender node with the transmission range $\mathcal{R}$ in a sector ϕ, given that there is at least one neighbor in the sector, is given by [29]

$$f_{\mathcal{R}}(\mathrm{r}) = \frac{\lambda\phi \mathrm{r} e^{\frac{\lambda\phi \mathrm{r}^2}{2}}}{e^{\lambda A}-1}, \qquad \text{for } 0 \le \mathrm{r} \le \mathcal{R}, \tag{33}$$

where $A = \frac{\phi\mathcal{R}^2}{2}$ is the area of the sector. In a PPP network with density λ, all the node distances of the route follow the same pdf. Thus, the mean hop length $\mathbb{E}[d]$ is given by

$$\mathbb{E}[d] = \frac{\mathcal{R}e^{\lambda A} - \sqrt{\frac{\pi}{2\lambda\phi}}\mathrm{erfi}\left(\mathcal{R}\sqrt{\lambda\phi/2}\right)}{e^{\lambda A}-1}, \tag{34}$$

where $\mathrm{erfi}(y) = \frac{2}{\sqrt{\pi}}\int_0^y e^{t^2}\, dt$ is the inverse error function. The proof is given in [29].

Further, the angle ω_k from the origin to the k^{th} node follows a Gaussian distribution with variance $V(\phi,k) \approx \phi^2/12k$ [30]. Thus, the path efficiency[5] of the selected nodes in farthest neighbor routing scheme is given by [32]

$$\overline{\eta(\omega)} \approx \left(1 - \frac{\phi^2}{24\lambda A}\right)\left(1-e^{-\lambda A}\right) + \frac{\phi^2}{24}e^{-\lambda A}. \tag{35}$$

Therefore, the average number of hops N of the routing protocol is given by

$$N = \frac{D_{S,D}}{\mathbb{E}[d]\overline{\eta(\omega)}}. \tag{36}$$

[5]The path efficiency is the ratio of the Euclidean distance between the end nodes and the actual distance travelled.

Next, we determine the average distance between any pair of sender/receiver nodes and the relay node. For each hop of the route, the relay node may be selected by the condition (18), (22) or (25). The relay node and the receiver node must be located in transmission range of the sender node. The pdf of the distance between the relay node and the receiver node within the transmission range of the sender node is given by [33]

$$f_d(\mathrm{r}) = \frac{2\mathrm{r}}{\mathcal{R}^2}\left(\frac{2}{\pi}\cos^{-1}\left(\frac{\mathrm{r}}{2\mathcal{R}}\right) - \frac{\mathrm{r}}{\pi\mathcal{R}}\sqrt{1-\frac{\mathrm{r}^2}{4\mathcal{R}^2}}\right), \quad \text{for } 0 \le \mathrm{r} \le \mathcal{R}. \quad (37)$$

Similarly, the pdf of the distance between the sender node and the relay node is given by (37). Hence, the average distance between the relay node and the sender/receiver node is given by

$$\mathbb{E}[\mathrm{r}] = \int_0^{\mathcal{R}} \frac{4\mathrm{r}^2}{\pi\mathcal{R}^2}\cos^{-1}\left(\frac{\mathrm{r}}{2\mathcal{R}}\right) - \frac{2\mathrm{r}^3}{\pi\mathcal{R}^3}\sqrt{1-\frac{\mathrm{r}^2}{4\mathcal{R}^2}}d\mathrm{r}. \quad (38)$$

Power and Throughput Model for Class A: In Rayleigh fading channel, the single hop minimum power consumption for a node x transmitting to a node y, subject to a rate demand, over all the aggregated channels is given by

$$P_{x,y}^{\min} = \sum_{k=1}^{N_A}\int_0^{\infty} 1 - \exp\left[\frac{-\mu\left(2^{\frac{R_d^k}{\mathbb{P}_{acc}^k B_k}} - 1\right)\delta^2 L_{x,y}}{t}\right] dt, \quad (39)$$

where N_A is the number of aggregated channels, R_d^k is the rate demand of the k^{th} aggregated channel, and $L_{x,y}$ is the path loss which can be calculated using (34) or (38) for the direct or relay transmission scenario respectively, with the selected path loss model. Note that $\sum_{k=1}^{N_A} R_d^k \ge R_d$ which means the total capacity of all aggregated channels must be larger than or equal to the rate demand.

Proof: The proof of (39) is given in Appendix A.

The total capacity of all aggregated channels in Rayleigh fading environment is given by

$$C_{x,y} = \sum_{k=1}^{N_A}\int_0^{\infty} \exp\left[\frac{-\mu\left(2^{\frac{t}{\mathbb{P}_{acc}^k B_k}} - 1\right)\delta^2 L_{x,y}}{\mathcal{P}_k^a}\right] dt, \quad (40)$$

where $\mathcal{P}_k^a$ is the maximum allowed transmit power of the k^{th} channel.

Proof: The proof of (40) can be obtained in a similar way as described in Appendix A.

To evaluate the probability of transmitting data over the cooperative link, ρ, we need to evaluate the probability of a successful transmission, which is given by

$$\begin{aligned} p^{ss} &= \mathbb{P}[SNR \ge \gamma] \\ &= \mathbb{P}\left[|F_{x,y}|^2 \ge \frac{\gamma\delta^2 L_{x,y}}{P_{x,y}}\right] \\ &= \exp\left(\frac{-\mu\gamma\delta^2 L_{x,y}}{P_{x,y}}\right), \end{aligned} \quad (41)$$

where γ is the threshold SNR for successful data transmission. Therefore, we have

$$P_{x,y} = \frac{\mu\gamma\delta^2 L_{x,y}}{-\ln p^{ss}}. \quad (42)$$

Using (42), $C_{x,y}$ can be expressed as

$$C_{x,y} = \sum_{k=1}^{N_A} W_{x,y}^k \log_2\left(1 + \frac{\mu\gamma|F_{x,y}^k|^2}{-\ln p^{ss}}\right), \quad (43)$$

where $W_{x,y}^k$ is obtained from (11).

As the power consumption and capacity are calculated according to Shannon's Theorem, the node which provides the maximum capacity must provide the minimum transmit power. According to (22) and (43), the probability of transmitting data over the cooperative link, ρ_A, for *Class A* is given by (44) (see equation at the bottom of the page).

Using (19) and (44), the transmit power of link (x, y) by involving a relay node r is given by (45) (see equation at the bottom of the next page).

Subsequently, the end-to-end power consumption from the source node to the destination node is given by

$$P_{S,D}^{tx} = N P_{x,y}^{tx}, \quad (46)$$

where N is given by (36).

Next, using (23), the end-to-end throughput from the source node to the destination node is given by (47) (see equation at the bottom of the next page), where $C_{x,y}$ is the capacity of link (x, y) which is given by (40), and $C_{x,r,y}$ is the capacity of the cooperative link which is equal to $\min[C_{x,r}, C_{r,y}]$ according to (21).

$$\begin{aligned} \rho_A &= \mathbb{P}\left[C_{x,r,y} > C_{x,y}\right] = \mathbb{P}\left[C_{x,r} > C_{x,y}\right]\mathbb{P}\left[C_{r,y} > C_{x,y}\right] \\ &= \mathbb{P}\left[|F_{x,r}|^2 > \frac{\left(2^{\frac{C_{x,y}}{W_{x,r}}} - 1\right)\left(-\ln p_{x,r}^{ss}\right)}{\gamma\mu}\right]\mathbb{P}\left[|F_{r,y}|^2 > \frac{\left(2^{\frac{C_{x,y}}{W_{r,y}}} - 1\right)\left(-\ln p_{r,y}^{ss}\right)}{\gamma\mu}\right] \\ &= \exp\left[\frac{\left(2^{\frac{C_{x,y}}{W_{x,r}}} - 1\right)\left(-\ln p_{x,r}^{ss}\right) + \left(2^{\frac{C_{x,y}}{W_{r,y}}} - 1\right)\left(-\ln p_{r,y}^{ss}\right)}{\gamma}\right] \end{aligned} \quad (44)$$

Delay Model for Class B: We use ETX as a default metric for relay node selection in *Class B*. Recall that ETX is defined as $\mathcal{E} = 1/p^{ss}$, where p^{ss} is given by (41). Therefore, the ETX between node x and node y can be expressed as

$$\mathcal{E}_{x,y} = \exp\left[\alpha L_{x,y}\right], \tag{48}$$

where $\alpha = \mu\gamma\delta^2/P_{x,y}$. According to the condition (25), the probability of transmitting data over cooperative link for *Class B*, ρ_B can be expressed as

$$\rho_B = \frac{1}{2} + \frac{1}{2}\,\text{erf}\left[\frac{\ln \mathcal{E}_{x,y} - \mu'_{etx}}{\sqrt{2}\sigma'}\right], \tag{49}$$

where $\text{erf}(y) = \frac{2}{\sqrt{\pi}}\int_0^y e^{-t^2}\ dt$ is the error function, $\sigma'^2 = \ln\left(\frac{\exp(\alpha^2)-1}{2}+1\right)$ and $\mu'_{etx} = \ln 2 + \frac{1}{2}\left(\alpha^2 - \sigma'^2\right)$.

Proof: The proof of (49) is given in Appendix B.

Considering the collisions for control packets, the single hop delay without re-transmissions is given by

$$\Phi = \left[\frac{1-\min(\mathbb{P}^j_{acc})}{\min(\mathbb{P}^j_{acc})} + \left\lceil\frac{N_{data}L_{data}}{TR_d}\right\rceil - 1\right]T_s + \frac{N_{data}L_{data}}{R_d} + T_b, \tag{50}$$

where $\mathbb{P}^j_{acc}$ is given by (4) such that $j \in \mathcal{F}$, N_{data} is the number of data packets, L_{data} is the data packet size, T is the transmission time, R_d is the rate demand, and T_b is the average back-off time for control packets until successful transmission which is given by (51) (see equation at the bottom of the page), where T_{slot} is the back-off slot duration, and $\lambda\pi\mathcal{R}^2 - 1$ denotes the number of neigbors of a sender node.

Proof: The proof of (50) and (51) is given in Appendix C.

Using (26) and (27), the end-to-end delay from the source node to the destination node is given by

$$\Phi_{S,D} = N\left((1-\rho)\mathcal{E}_{x,y}\Phi_{x,y} + \rho\left(\mathcal{E}_{x,r}\Phi_{x,r} + \mathcal{E}_{r,y}\Phi_{r,y}\right)\right), \tag{52}$$

where N is given by (36), ρ_B is given by (49), and Φ is given by (50).

VI. Performance Evaluation

In this section, we analyse the performance of our proposed cooperative routing protocol. For the sake of validating the analytical results, we also perform a simulation study. We implement SACRP in MATLAB with the network topology as shown in Fig. 6. Other simulation parameters are given in Table II. A square region of side 1200 m is assumed with 9 PU transmitters. Each PU transmitter has 5 channels. Similar to the analytical model, we assume that the CR users are Poisson distributed in the whole region with a density $\lambda = 200$ nodes/km. The parameters characterizing the *ON* and *OFF* times of PU transmitters are randomly set in the interval $[0, 1]$. We consider

$$P^{tx}_{x,y} = \sum_{k=1}^{N_A}\left(1-\exp\left[\frac{\left(2^{\frac{C_{x,y}}{W_{x,r}}}-1\right)\left(-\ln p^{ss}_{x,r}\right) + \left(2^{\frac{C_{x,y}}{W_{r,y}}}-1\right)\left(-\ln p^{ss}_{r,y}\right)}{\gamma}\right]\right)\int_0^\infty 1-\exp\left[-\mu\frac{\left(2^{\frac{R^k_d}{\mathbb{P}^k_{acc}B_k}}-1\right)\delta^2 L_{x,y}}{t}\right]dt$$
$$+\left(\sum_{n=1}^{N'_A}\int_0^\infty 1-\exp\left[-\mu\frac{\left(2^{\frac{R^n_d}{\mathbb{P}^n_{acc}B_n}}-1\right)\delta^2 L_{x,r}}{t}\right]dt + \sum_{m=1}^{N''_A}\int_0^\infty 1-\exp\left[-\mu\frac{\left(2^{\frac{R^m_d}{\mathbb{P}^m_{acc}B_m}}-1\right)\delta^2 L_{r,y}}{t}\right]dt\right)$$
$$\times\exp\left[\frac{\left(2^{\frac{C_{x,y}}{W_{x,r}}}-1\right)\left(-\ln p^{ss}_{x,r}\right) + \left(2^{\frac{C_{x,y}}{W_{r,y}}}-1\right)\left(-\ln p^{ss}_{r,y}\right)}{\gamma}\right]. \tag{45}$$

$$\Theta = \left((1-\rho)\left(1-\mathbb{P}_{RTS}\right)\left(1-\mathbb{P}_{CTS}\right)\left(1-\mathbb{P}_{RES}\right)p^{ss}_{x,y}\right)^N C_{x,y} + \left(\left(\rho\left(1-\mathbb{P}_{RTS}\right)\left(1-\mathbb{P}_{CTS}\right)\left(1-\mathbb{P}_{RES}\right)\right)^2 p^{ss}_{x,r}p^{ss}_{r,y}\right)^N C_{x,r,y}. \tag{47}$$

$$T_b = \left(\frac{1}{\left(1-\mathbb{P}_{RTS}\right)\left(1-\mathbb{P}_{CTS}\right)\left(1-\mathbb{P}_{RES}\right)\left[1-\left[\left(1-\mathbb{P}_{RTS}\right)\left(1-\mathbb{P}_{CTS}\right)\left(1-\mathbb{P}_{RES}\right)\right]^{\frac{1}{\lambda\pi\mathcal{R}^2-1}}\right]} - 1\right)T_{slot}, \tag{51}$$

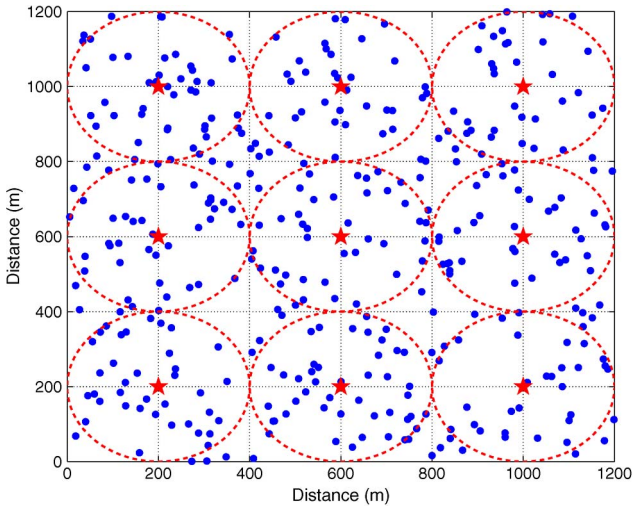

Fig. 6. Simulated network topology. The stars and dotted circles represent the location and coverage area of PU transmitters, respectively. The dots represent the location of CR users.

TABLE II
SIMULATION PARAMETERS

Parameter	Value
Range of Frequency Bands	3 bands each in 900 MHz, 1800 MHz and 2100 MHz
Detection probability threshold ($\mathbb{P}_d^{'}$)	0.9
Probability of false alarm ($\mathbb{P}_f$)	0.1
Channel bandwidth	2 MHz
Maximum Interference Ratio (IR_{max})	0.25
Spectrum sensing duration (T_s)	20 ms
Back-off slot duration(T_{slot})	20 μs
Transmission time of a data packet (T)	60 ms
Maximum transmit power ($\mathcal{P}_{max}$)	30 dBm
Maximum allowed transmit power ($\mathcal{P}^a$)	20 dBm
PU transmission range ($\mathcal{R}_{PU}$)	200 m
CR node transmission range ($\mathcal{R}_{CR}$)	150 m
Antenna height	15 m
Transmission rate demand (R_d)	512 kbps
Number of data packets (N_{data})	100
Data Packet size (L_{data})	1000 bytes
Path loss model	Okumura model [34] applicable for 150-3000 MHz

a frequency selective Rayleigh fading channel between any two nodes, where the channel gain accounts for Rayleigh fading and path loss.

Firstly, we validate the analytical results. Fig. 7 shows the end-to-end power consumption against the network density. As shown, the transmission power decreases when the network density increases. This is because the probability of finding a relay node increases with the network density. Moreover, the end-to-end power consumption in high frequency band is larger than that of the low frequency band, as the high frequency band suffers more path loss. In addition, for a given probability of PU being active, P_b, the power consumption is reduced when the number of aggregated channels increases due to the infamous bandwidth-power inverse relationship. The power consumption increases as P_b increases due to the fact that a higher PU activity will reduce the potentially available bandwidth. Note that the simulation results closely follow the analytical results and hence validate the analytical modeling.

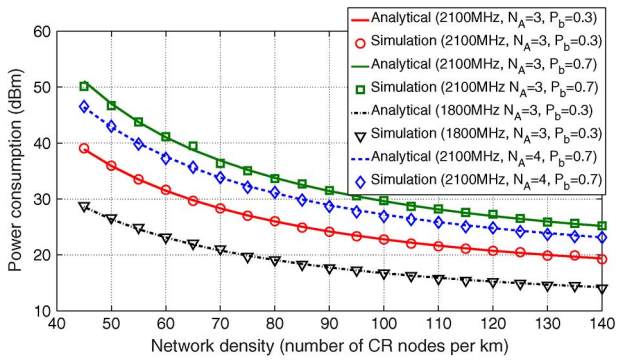

Fig. 7. End-to-end power consumption against network density in SACRP N_A is the number of aggregated channels, and P_b is the PU activity.

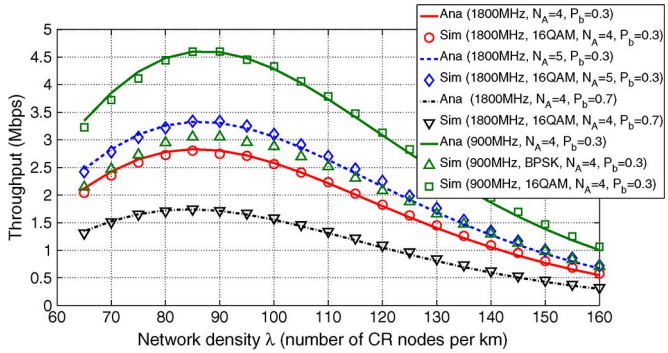

Fig. 8. End-to-End throughput against network density in SACRP, N_A is the number of aggregated channels, and P_b is the PU activity.

The analytical and simulation results for the end-to-end throughput are given in Fig. 8. It is noted that the throughput initially increases and then decreases with the network density. This is because the probability of finding a relay node, which provides higher capacity, increases with the network density. On the other hand, the probability of control packet collision also increases with the network density; as a result of which the throughput degrades. Besides, the low frequency band provides higher throughput than the high frequency band due to the fact that the latter suffers more path loss. As expected, for a given P_b, the end-to-end throughput increases with the number of aggregated channels. Furthermore, the end-to-end throughput decreases with higher PU activity. We also note that increasing the order of modulation in simulations achieves higher throughput, which is intuitive. Moreover, higher order modulation performs close to the analytical results.

Fig. 9 depicts the end-to-end delay against the network density. We vary the ETX of the cooperative link and note that the relay node provides lower end-to-end delay in good channel conditions (i.e., low ETX). Moreover, the end-to-end delay initially decreases and then increases as the network density increases. This is because the probability of finding a relay node, providing lower ETX, increases with the network density. However, the probability of control packet collision also increases with the network density, which increases the number of re-transmissions. In addition, the end-to-end delay increases with higher PU activity as the effective transmission time for a CR node is reduced. As before, the simulation results

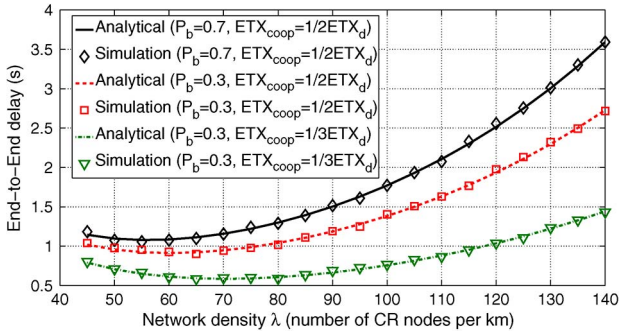

Fig. 9. End-to-End delay against network density in SACRP, P_b is the PU activity.

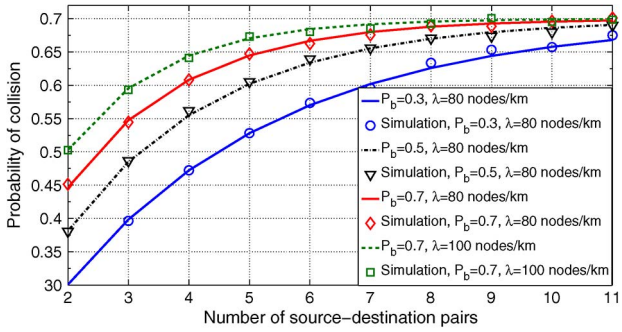

Fig. 10. The probability of collision against the number of source and destination pairs, λ is the network density, P_b is the PU activity.

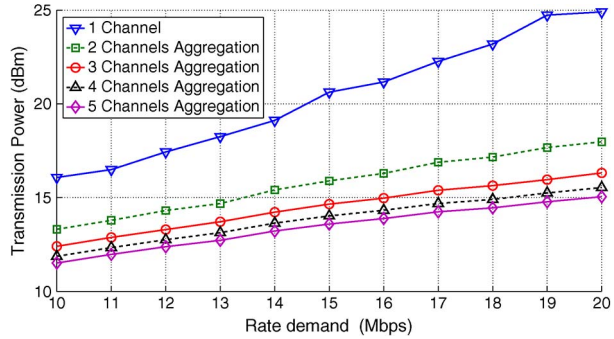

Fig. 11. Transmission power consumption against the rate demand in SACRP *Class A*.

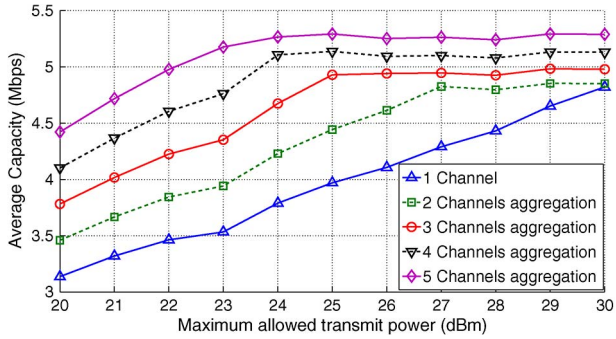

Fig. 12. Average capacity performance against the maximum allowed transmit power of each channel ($\mathcal{P}^a$) in SACRP *Class A*.

closely follow the analytical results and hence validate the analytical modeling.

The analytical and simulation results for the cumulative probability of collision (for all types of control packets) against the number of source-destination pairs are shown in Fig. 10. It can be seen that the probability of collision increases with the the number of source-destination pairs. For a given network density, the probability of collision increases with higher PU activity. This is due to the reduction in effective resources (shared by all CR nodes) for the transmission of CR nodes. Besides, for a given P_b, a higher network density will result in higher probability of collision. As before, the simulation results closely follow the analytical results and hence validate the analytical modeling.

After validating the analytical results with simulations, we conduct a simulation-based performance evaluation and a performance comparison of the proposed routing protocol.

Firstly, we evaluate the performance of transmit power consumption in our proposed *Class A* protocol. Fig. 11 depicts the transmit power as a function of the rate demand between the source and the destination. As the rate demand increases, the power consumption also increases. As shown, our proposed *Class A* can reduce the transmit power significantly. The transmit power is further reduced as more channels are aggregated. However, as the number of aggregated channels increases, the transmit power gain is decreased. As shown in Fig. 11, the maximum gain is achieved with two aggregated channels. This is because the CR node has to overcome more attenuation (path loss and fading) of the aggregated channels when the number of aggregated channels increases.

The average capacity performance against the maximum allowed transmit power of each channel ($\mathcal{P}^a$) is shown in Fig. 12. In this case, we assume that the $\mathcal{P}^a$ of each channel is fixed and increases from 20 dBm to 30 dBm. The maximum power constraint P_{max} of each CR node is set as 30 dBm. With the increase in $\mathcal{P}^a$, the capacity performance increases. The capacity performance reaches a saturation point as soon as the total transmission power reaches the constraint P_{max}.

Next, we compare our proposed SACRP with other protocols with spectrum aggregation in the same simulation configurations. We assume that the MSA spectrum aggregation algorithm [8] is combined with non-cooperative Routing Protocol: CRP-*Class I* [16] and cooperative routing protocol: COOP [17], respectively.

Fig. 13 presents the transmit power performance as a function of the distance between the source and the destination. We observe that the transmit power grows with the distance. Our proposed *Class A* costs the minimum transmit power compared with other three protocols. Both *Class A* and *Class B* have better performance than other protocols. This is because *Class A* always aggregates the channels which can provide the minimum transmit power. For different channel quality, it is able to adjust the transmit power to reduce the overall power consumption. Moreover, *Class B* aggregates channels that provide more effective transmission time, which increases the potential capacity and therefore reduces the transmit power.

From Fig. 14, it can be seen that the *Class A* protocol achieves the maximum throughput performance. In this case, *Class A* aggregates the spectrum channels which have the maximum capacity and adjusts the transmit power under the

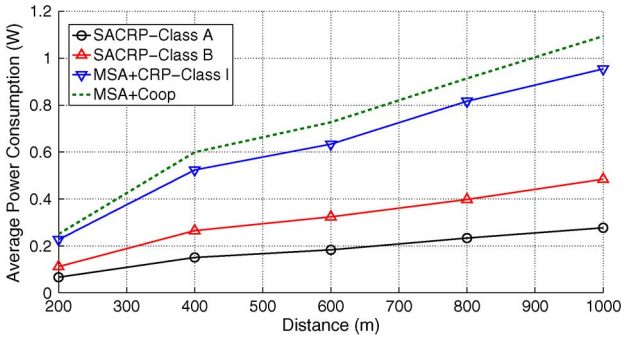

Fig. 13. Transmit power consumption against the distance between the source and destination.

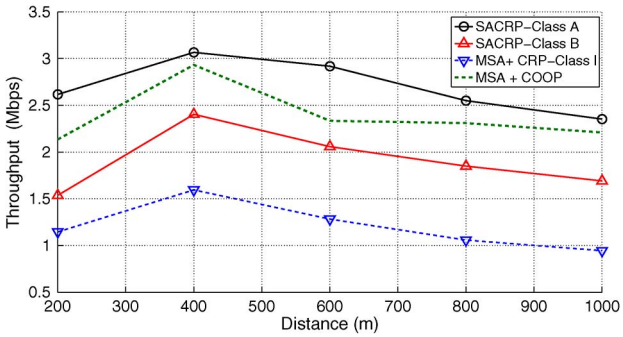

Fig. 14. Throughput against the distance between the source and destination.

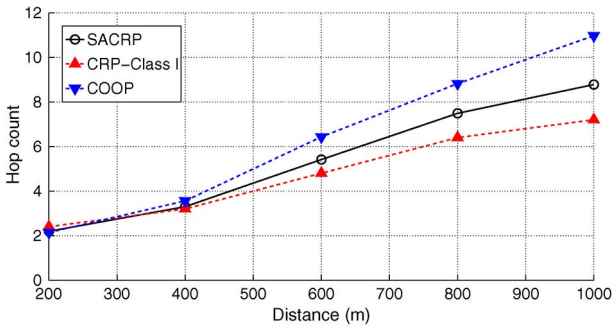

Fig. 15. Hop count against the distance between the source and destination.

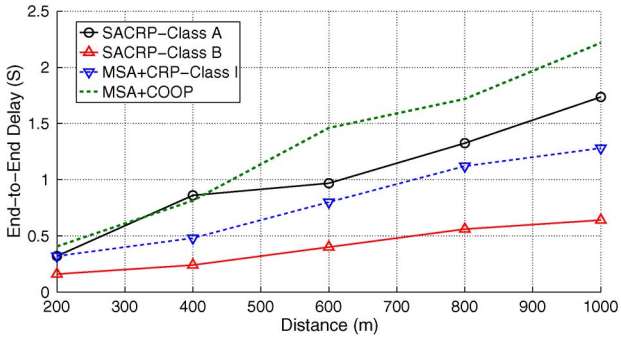

Fig. 16. The end-to-end delay against the distance between the source and destination.

power constraints to achieve high throughput. However, MSA algorithm only aggregates the channels which satisfy the bandwidth requirements. It does not consider the channel quality and power control. Notice that, the throughput performance of *Class B* is better than that of the MSA with CRP-*Class I*. This is due to higher effective transmission time and cooperative link selection with better ETX.

Last, but not least, we also evaluate the delay performance of our proposed protocol. In Fig. 15, we consider the hop count performance. It is clear that our proposed SACRP incurs less hop count than COOP, but has a larger hop count compared to CRP-*Class I*. This is because SACRP selects the route which has the minimum hop count; however, the cooperative link will increase the number of hops. As shown in Fig. 16, SACRP *Class B* results in the minimum end-to-end delay. Even though it's hop count is larger than CRP-*Class I*, more effective transmit time provided by direct link and less number of retransmissions provided by the cooperative link are able to reduce the end-to-end delay significantly. We note that MSA with COOP shows the worst performance as it cannot guarantee the effective transmit time for aggregated spectrum bands. In addition, COOP generates larger number of hops than SACRP.

VII. Conclusion

In this paper, we have proposed SACRP, which is a spectrum aggregation-based cooperative routing protocol for CRAHNs. SACRP considers two classes of cooperative routing protocols: *Class A* for power minimization or throughput maximization, and *Class B* for reducing the end-to-end delay. A stochastic geometry approach has been used to develop the analytical model for the proposed protocol. Performance evaluation demonstrate that *Class A* aggregates multiple channels and selects suitable relay nodes, and therefore achieves higher power efficiency and throughput. *Class B* reduces the number of re-transmissions by selecting the relay nodes with better channel conditions, and therefore reduces the end-to-end delay. We have also conducted a performance comparison of SACRP with other relevant protocols in literature. Results shows that SACRP *Class A* reduces the transmit power by up to 70% compared to MSA in cooperative as well well as non-cooperative scenarios. Apart from this it enhances the overall throughput by up to 50% and 20% compared to MSA in non-cooperative and cooperative scenarios, respectively. Besides, SACRP *Class B* reduces the end-to-end delay by up to 38% and 55% compared to MSA in non-cooperative and cooperative scenarios respectively. For future work, we aim to investigate the applicability of SACRP for network reliability and PU receiver protection.

Appendix A
Proof of (39)

Based on Shannon's Theorem, the total transmission power for aggregating N_A channels is given by

$$P_{x,y}^{min} \triangleq \mathbb{E}\left[\sum_{k=1}^{N_A} \frac{\left(2^{\frac{R_d^k}{\mathbb{P}_{acc}^k B_k}} - 1\right)\delta^2}{|h_{x,y}^k|^2}\right],$$

where $|h^k_{x,y}|^2 = |F^k_{x,y}|^2/L_{x,y}$. Note that all aggregated channels are independent and identically distributed (i.i.d). In Rayleigh fading environments, $|F^k_{x,y}|^2 \sim \text{Exp}(\mu)$. Note that for a random variable X taking non-negative values, the expected value can be calculated using the complementary Cumulative Distribution Function (CDF) i.e., $\mathbb{E}[X] = \int_{t>0} \mathbb{P}(X > t)\ dt$. Therefore,

$$\begin{aligned} P^{min}_{x,y} &\triangleq \mathbb{E}\left[\sum_{k=1}^{N_A} \frac{\left(2^{\frac{R^k_d}{\mathbb{P}^k_{acc} B_k}} - 1\right)\delta^2 L_{x,y}}{|F^k_{x,y}|^2}\right] \\ &= \sum_{k=1}^{N_A} \mathbb{E}\left[\frac{\left(2^{\frac{R^k_d}{\mathbb{P}^k_{acc} B_k}} - 1\right)\delta^2 L_{x,y}}{|F^k_{x,y}|^2}\right] \\ &= \sum_{k=1}^{N_A} \int_{t>0} \mathbb{P}\left(\frac{\left(2^{\frac{R^k_d}{\mathbb{P}^k_{acc} B_k}} - 1\right)\delta^2 L_{x,y}}{|F^k_{x,y}|^2} > t\right) dt \\ &= \sum_{k=1}^{N_A} \int_{t>0} \mathbb{P}\left(|F^k_{x,y}|^2 < \frac{\left(2^{\frac{R^k_d}{\mathbb{P}^k_{acc} B_k}} - 1\right)\delta^2 L_{x,y}}{t}\right) dt \\ &= \sum_{k=1}^{N_A} \int_0^{\infty} 1 - \exp\left[-\mu \frac{\left(2^{\frac{R^k_d}{\mathbb{P}^k_{acc} B_k}} - 1\right)\delta^2 L_{x,y}}{t}\right] dt, \end{aligned} \tag{53}$$

which completes the proof.

Appendix B
Proof of (49)

According to (25), we have $\rho = \mathbb{P}[\mathcal{E}_{x,r} + \mathcal{E}_{r,y} < \mathcal{E}_{x,y}]$. From (48), we have $\mathcal{E}_{x,y} = \exp[\alpha L_{x,y}]$, where $\alpha = \mu\gamma\delta^2/P_{x,y}$. In this case, μ, γ, and δ^2 are constant for all CR nodes. Under the assumption of fixed transmission power $P_{x,y}$, ETX ($\mathcal{E}$) is a log-normal distributed with mean $\mu_{etx} = 0$ and variance $\sigma^2 = \alpha^2$. Using the substitution $X \to \mathcal{E}_{x,r}$ and $Y \to \mathcal{E}_{r,y}$, we have $\rho = \mathbb{P}[X + Y < \mathcal{E}_{x,y}]$.

The probability of finding the relay node for *Class B* requires the pdf of a sum of two log-normal random variables. As X and Y have the same mean and variance, the pdf can be found using the Fenton-Wilkinson (FW) approximation [35], according to which the random variable $X + Y$ is also log-normally distributed with mean $\mu'_{etx} = \ln 2 + \frac{1}{2}\left(\sigma^2 - \sigma'^2\right)$, where σ'^2 is the variance and is given by $\sigma'^2 = \ln\left(\frac{\exp(\sigma^2)-1}{2} + 1\right)$.

The CDF for the log-normal distributed random variable g having mean μ_g and variance σ^2_g is given by

$$\frac{1}{2} + \frac{1}{2}\ \text{erf}\left[\frac{\ln g - \mu_g}{\sqrt{2}\sigma_g}\right].$$

Changing $g \to \mathcal{E}_{s,d}$, $\mu_g \to \mu'_{etx}$ and $\sigma^2_g \to \sigma'^2$, we have the probability ρ_B in (49). This completes the proof.

Appendix C
Proof of (50)

Note that the delay for a single hop for a single transmission can be expressed by $\Phi = N_{ss}T_s + T_t + T_b$, where N_{ss} is the number of spectrum sensing events, T_s is the spectrum sensing duration, T_t is the total time for transmitting data packets, and T_b is the average back-off time for control packets until sucessful transmission.

Let $\mathbb{P}_n$ denote the probability that a CR node will successfully transmit data after n spectrum sensing times. Thus, $\mathbb{P}_n$ is given by

$$\mathbb{P}_n = (1 - \mathbb{P}_{acc})^n \mathbb{P}_{acc}. \tag{54}$$

Let n_s be the random variable that represents the total number of spectrum sensing events until success. Since $\mathbb{P}_n$ represents the Probability Mass Function (PMF) of n_s, the average number of spectrum sensing events until success is given by

$$N_s = \mathbb{E}(n_s) = \sum_{n=0}^{\infty} n\mathbb{P}_n = \frac{1 - \mathbb{P}_{acc}}{\mathbb{P}_{acc}}. \tag{55}$$

where $\mathbb{P}_{acc} = \min(\mathbb{P}^j_{acc})$ due to the data packets are split and transmitted simutaneously over the aggregated channels.

Note that if $T_t > T$, the CR node cannot transmit all data packets within the duration of one transmission time T. Hence, the total number of spectrum sensing events N_{ss} can be calculated by

$$N_{ss} = N_s + \left\lceil \frac{N_{data}L_{data}}{TR_d} \right\rceil - 1, \tag{56}$$

where N_{data} is the number of data packets, R_d is the rate demand, and L_{data} is the data packet size.

Next, using a similar methodology as employed for calculating the average number of spectrum sensing events, the average number of collisions for control packets until successful transmission N_c is given by

$$N_c = \frac{\mathbb{P}_c}{1 - \mathbb{P}_c} = \frac{1 - (1 - \mathbb{P}_{RTS})(1 - \mathbb{P}_{CTS})(1 - \mathbb{P}_{RES})}{(1 - \mathbb{P}_{RTS})(1 - \mathbb{P}_{CTS})(1 - \mathbb{P}_{RES})}. \tag{57}$$

where $\mathbb{P}_c$ is the probability that a collision for control packets occurs owing to simultaneous transmission from multiple nodes. It should be noted that Geometric distribution has been employed to compute N_c, similar to the analysis in [36].

Thus, the expected backoff time T_b (which can be calculated according to (27) in [36]) is given by

$$T_b = N_e T_{slot} = \left(\frac{N_c + 1}{\mathbb{P}_t} - 1\right) T_{slot}, \tag{58}$$

where N_e is the expected number of back-off time slots, T_{slot} is the duration of back-off time slot, and $\mathbb{P}_t = 1-(1-\mathbb{P}_c)^{1/(\lambda\pi\mathcal{R}^2-1)}$ denotes the probability that a given node will transmit in an arbitrary time slot which is also given by [36]. Therefore, Φ is given by (50). This completes the proof.

ACKNOWLEDGMENT

The authors thank the editor and the reviewers for healthy criticism and valuable suggestions that led to significant improvements in this paper.

REFERENCES

[1] C. Li, W. Liu, J. Li, Q. Liu, and C. Li, "Aggregation based spectrum allocation in cognitive radio networks," in *Proc. IEEE/CIC ICCC Workshops*, 2013, pp. 50–54.
[2] I. F. Akyildiz, W.-Y. Lee, M. C. Vuran, and S. Mohanty, "NeXt generation/dynamic spectrum access/cognitive radio wireless networks: A survey," *Comput. Netw.*, vol. 50, no. 13, pp. 2127–2159, Sep. 2006.
[3] M. Nekovee, "Quantifying the availability of TV white spaces for Cognitive Radio operation in the U.K.," in *Proc. IEEE ICC Workshops*, 2009, pp. 1–5.
[4] I. F. Akyildiz, W.-Y. Lee, and K. R. Chowdhury, "CRAHNs: Cognitive radio ad hoc networks," *Ad Hoc Netw.*, vol. 7, no. 5, pp. 810–836, Jul. 2009.
[5] P. Ren, Y. Wang, Q. Du, and J. Xu, "A survey on dynamic spectrum access protocols for distributed cognitive wireless networks," *EURASIP J. Wireless Commun. Netw.*, vol. 2012, p. 60, 2012.
[6] W. Wang, Z. Zhang, and A. Huang, "Spectrum aggregation: Overview and challenges," *Netw. Protocols Algorithms*, vol. 2, no. 1, pp. 184–196, 2010.
[7] B. Gao, Y. Yang, and J. Park, "Channel aggregation in cognitive radio networks with practical considerations," in *Proc. IEEE ICC*, 2011, pp. 1–5.
[8] F. Huang, W. Wang, H. Luo, G. Yu, and Z. Zhang, "Prediction-based spectrum aggregation with hardware limitation in cognitive radio networks," in *Proc. IEEE VTC*, 2010, pp. 1–5.
[9] H. Salameh, M. Krunz, and D. Manzi, "Spectrum bonding and aggregation with guard-band awareness in cognitive radio networks," *IEEE Trans. Wireless Commun.*, vol. 13, no. 3, pp. 569–581, Mar. 2014.
[10] D. Chen, Q. Zhang, and W. Jia, "Aggregation aware spectrum assignment in cognitive Ad-hoc networks," in *Proc. CROWNCOM*, 2008, pp. 1–6.
[11] J. Lin *et al.*, "Channel characteristic aware spectrum aggregation algorithm in cognitive radio networks," in *Proc.IEEE LCN*, 2011, pp. 634–639.
[12] J. Poston and W. Horne, "Discontiguous OFDM considerations for dynamic spectrum access in idle TV channels," in *Proc. IEEE DySPAN*, 2005, pp. 607–610.
[13] H. Rahul, F. Edalat, D. Katabi, and C. Sodini, "Frequency-aware rate adaptation and MAC protocols," in *Proc. ACM MobiCom*, 2009, pp. 193–204.
[14] S. Salim and S. Moh, "On-demand routing protocols for cognitive radio ad hoc networks," *EURASIP J. Wireless Commun. Netw.*, vol. 2013, p. 102, 2013.
[15] Y. Liu, L. Cai, and X. Shen, "Spectrum-aware opportunistic routing in multi-hop cognitive radio networks," *IEEE J. Sel. Areas Commun.*, vol. 30, no. 10, pp. 1958–1968, Nov. 2012.
[16] K. R. Chowdhury and I. F. Akyildiz, "CRP: A routing protocol for cognitive radio ad hoc networks," *IEEE J. Sel. Areas Commun.*, vol. 29, no. 4, pp. 794–804, Apr. 2011.
[17] J.-P. Sheu and I.-L. Lao, "Cooperative routing protocol in cognitive radio ad-hoc networks," in *Proc. IEEE WCNC*, 2012, pp. 2916–2921.
[18] D. Lei, T. Melodia, S. Batalama, and J. Matyjas, "Distributed routing, relay selection, and spectrum allocation in cognitive and cooperative ad hoc networks," in *Proc. IEEE SECON*, 2010, pp. 1–9.
[19] J. Jia, J. Zhang, and Q. Zhang, "Cooperative relay for cognitive radio networks," in *Proc. IEEE INFOCOM*, 2009, pp. 2304–2312.
[20] S. You, S. Misra, T. Lang, and E. Anthony, "Cooperative routing for distributed detection in large sensor networks," *IEEE J. Sel. Areas Commun.*, vol. 25, no. 2, pp. 471–483, Feb. 2007.
[21] S. Ping, A. Aijaz, O. Holland, and A. Aghvami, "Energy and interference aware cooperative routing in cognitive radio ad-hoc networks," in *Proc. IEEE WCNC*, Apr. 2014, pp. 87–92.
[22] J. Jia and S. Zhang, "Cooperative transmission in cognitive radio ad hoc networks," *Int. J. Distrib. Sensor Netw.*, vol. 2012, 2012, Art. ID. 863634.
[23] P. aramvir Bahl, R. Chandra, T. Moscibroda, R. Murty, and M. Welsh, "White space networking with wi-fi like connectivity," in *Proc. ACM SIGCOMM*, Aug. 2009, pp. 27–38.
[24] P. Ren, Y. Wang, and Q. Du, "CAD-MAC: A channel-aggregation diversity based mac protocol for spectrum and energy efficient cognitive ad hoc networks," *IEEE J. Sel. Areas Commun.*, vol. 32, no. 2, pp. 237–250, Jan. 2014.
[25] H. Urkowitz, "Energy detection of deterministic signals," *Proc. IEEE*, vol. 55, no. 4, pp. 523–531, Apr. 1967.
[26] A. Ghasemi and E. S. Sousa, "Optimization of spectrum sensing for opportunistic spectrum access in cognitive radio networks," in *Proc. IEEE CCNC*, 2007, pp. 1022–1026.
[27] W.-Y. Lee and I. Akyildiz, "Optimal spectrum sensing framework for cognitive radio networks," *IEEE Trans. Wireless Commun.*, vol. 7, no. 10, pp. 3845–3857, Oct. 2008.
[28] D. S. J. De Couto, D. Aguayo, J. Bicket, and R. Morris, "A high-throughput path metric for multi-hop wireless routing," in *Proc. MobiCom*, 2003, pp. 134–146.
[29] M. Haenggi, "On distances in uniformly random networks," *IEEE Trans. Inf.Theory*, vol. 51, no. 10, pp. 3584–3586, Oct. 2005.
[30] M. Haenggi, "On routing in random rayleigh fading networks," *IEEE Trans. Wireless Commun.*, vol. 4, no. 4, pp. 1553–1562, Jul. 2005.
[31] H. ElSawy, E. Hossain, and M. Haenggi, "Stochastic geometry for modeling, analysis, and design of multi-tier and cognitive cellular wireless networks: A survey," *IEEE Commun. Surveys Tuts.*, vol. 15, no. 3, pp. 996–1019, 3rd Quart. 2013.
[32] M. Xie, W. Zhang, and K.-K. Wong, "A geometric approach to improve spectrum efficiency for cognitive relay networks," *IEEE Trans. Wireless Commun.*, vol. 9, no. 1, pp. 268–281, Jan. 2010.
[33] D. Moltchanov, "Survey paper: Distance distributions in random networks," *Ad Hoc Netw.*, vol. 10, no. 6, pp. 1146–1166, Aug. 2012.
[34] J. S. Seybold, *Introduction to RF propagation*. Hoboken, NJ, USA: Wiley, 2005.
[35] L. Fenton, "The sum of log-normal probability distributions in scatter transmission systems," *IRE Trans. Commun. Syst.*, vol. 8, no. 1, pp. 57–67, Mar. 1960.
[36] B.-J. Kwak, N.-O. Song, and M. Miller, "Performance analysis of exponential backoff," *IEEE/ACM Trans. Netw.*, vol. 13, no. 2, pp. 343–355, Apr. 2005.

Shuyu Ping received the bachelor's degree and became a graduate student in e-commerce engineering with law: a joint programme between Beijing University of Posts and Telecommunications (BUPT) and Queen Mary University of London (QMUL) in 2011. He received the M.Sc. degree (with distinction) in mobile and personal communications from King's College London in 2012. He is pursuing the Ph.D. degree at the Centre for Telecommunications Research, King's College London. His research interests include cognitive radio networks, cellular networks, and wireless sensor networks.

Adnan Aijaz (M'14) received the B.E. degree in electrical (telecom) engineering from National University of Sciences and Technology (NUST), Pakistan. He also received the M.Sc. degree in mobile and personal communications and the Ph.D. degree in telecommunications engineering from King's College London, in October 2011 and October 2014, respectively. Currently, he is working as a Research Associate with the Centre for Telecommunications Research, King's College London. His research interests include 5G cellular networks, machine-to-machine communications, full-duplex communications, cognitive radio networks, smart grids, and molecular communications.

Prior to joining King's, he worked in cellular industry for nearly 2.5 years in the areas of network performance management, optimization, and quality assurance.

Oliver Holland received the B.Sc. degree with first class honors from Cardiff University and the Ph.D. degree from King's College London. He is a Research Fellow at King's College London. He led the ICT-ACROPOLIS Network of Excellence (www.ict-acropolis.eu) until that project completed in December 2013, and he is currently leading a major trial of TV white spaces technology as part of the Ofcom TV White Spaces Pilot. He is a Leadership Member of the IEEE Dynamic Spectrum Access Networks Standards Committee (DySPAN-SC), is Chair and member of IEEE 1900.1, Chair and member of IEEE 1900.6, and Vice-Chair and member of IEEE 1900.7. He was a Technical Editor of the IEEE 1900.4 standard, the IEEE 1900.1a standard, and the IEEE 1900.6a standard. He was a Management Committee member representing the U.K. for the recently completed COST Actions IC0902 and IC0905 TERRA, holding various leadership positions therein. He has served on the TPCs of all major conferences in the area of mobile and wireless communications, has served as Invited (Keynote) Speaker, Session Chair and Panellist at numerous international conferences and events covering green radio and cognitive radio, among other topics, and frequently serves as reviewer for various prestigious international conferences and journals. He has assumed leadership positions in numerous international workshops, conferences, and journals. Dr. Holland is an Editor of IEEE TVT, and is an Officer of the IEEE Technical Committee on Cognitive Networks (TCCN) serving as Secretary and as Liaison between TCCN and DySPAN-SC. He is currently Chair of the UKRI Chapter of the IEEE VTS. He has co-authored over 140 publications, of which over 130 have been located on Google Scholar more than 850 times.

Abdol-Hamid Aghvami (M'89–SM'91–F'05) is a Professor of telecommunications engineering at King's College London. He has published over 600 technical papers and given invited talks and courses worldwide on various aspects of personal and mobile radio communications. He was Visiting Professor at NTT Radio Communication Systems Laboratories in 1990, Senior Research Fellow at BT Laboratories in 1998–1999, and was an Executive Advisor to Wireless Facilities Inc., USA, in 1996–2002. He was a member of the Board of Governors of the IEEE Communications Society in 2001–2003, was a Distinguished Lecturer of the IEEE Communications Society in 2004–2007, and has been member, Chairman, and Vice-Chairman of the technical programme and organising committees of a large number of international conferences. He is also the founder of International Symposium on Personal Indoor and Mobile Radio Communications (PIMRC), a major yearly conference attracting nearly 1000 attendees.

Dr. Aghvami was awarded the IEEE Technical Committee on Personal Communications (TCPC) Recognition Award in 2005 for his outstanding technical contributions to the communications field, and for his service to the scientific and engineering communities. He is a Fellow of the Royal Academy of Engineering, Fellow of the IET, and in 2009 was awarded a Fellowship of the Wireless World Research Forum in recognition of his personal contributions to the wireless world.